



STRUCTURAL
BIOLOGY

Volume 79 (2023)

Supporting information for article:

Structural basis of DNA binding by YdaT, a functional equivalent of the CII repressor in the cryptic prophage CP-933P from *Escherichia coli* O157:H7

Maruša Prolič-Kalinšek, Alexander N. Volkov, San Hadži, Jeroen Van Dyck, Indra Bervoets, Daniel Charlier and Remy Loris

Table S1 Primers used for cloning, EMSA and to generate the fragment used for footprinting

primer	sequence 5' -> 3'
1	AGCCACAGTTAAGAACATTACCGTGAGATCGTCGA
2	TAATATTCTTAACTGTGGCTGCGCATACGGGC
3	GGGATCGGAACGTGAAGGATGTCGATGATCGTGTGCGTCAGCGGTTGTTGTATGAC
4	ACGCAACACGATCATCGACATCCTCACGTTCCGATCCCTCCGTTGACGATCTCACGG
5	TTCGCAGCCGGTACTTTTC
6	GGAGCTACGACCCCCATGATT
7	ATTCCCAGCTCGAAATACGCT

Table S2 Crystallographic data collection and dataprocessing

Values for the outer shell are given in parentheses.

(a) Data collection and scaling using XDS	
Diffraction source	Soleil Proxima 1,
Wavelength (Å)	0.976
Temperature (K)	100
Detector	EIGER X 9M
Crystal-detector distance (mm)	331.98
Rotation range per image (°)	0.1
Total rotation range (°)	240
Space group	P1
a, b, c (Å)	45.57, 64.26, 63.91
α, β, γ (°)	66.83, 89.36, 77.67
Mosaicity (°)	0.193
Resolution range (Å)	44.37 - 2.40 (2.52-2.40)
(b) Anisotropic scaling using Staraniso	
Ellipsoidal resolution (Å)	
along 0.880 a * + 0.221 b * - 0.420 c *	2.23
along 0.072 a * + 0.854 b * + 0.515 c *	2.40
along 0.292 a * - 0.214 b * + 0.932 c *	2.90
Wilson B-factor (Å ²)	
along 0.856 a * + 0.296 b * - 0.424 c *	34.79
along 0.012 a * + 0.887 b * + 0.462 c *	54.93
along 0.323 a * - 0.043 b * + 0.946 c *	103.30
Completeness (spherical)	77.4 (32.5)
Completeness (ellipsoidal)	90.9 (72.8)
R _{merge}	0.082 (0.386)
R _{meas}	0.106 (0.552)
CC(1/2)	0.990 (0.797)
Total No. of reflections	45947 (2046)
No. of unique reflections	19698 (993)
$\langle I/\sigma(I) \rangle$	6.0 (1.4)

Table S3 Crystallographic structure solution and refinement

Resolution range (Å)	44.40 - 2.40 (2.52- 2.40)
σ cutoff	none
No. of reflections, working set	18719
No. of reflections, test set	979
Final R_{cryst}	0.2112 (0.2757)
Final R_{free}	0.2658 (0.2783)
No. of non-H atoms	
Protein	3757
Other	154
R.m.s. deviations	
Bond lengths (Å)	0.0088
Bond angles (°)	0.959
Chirality	0.052
Clashscore	5.83
Planar groups	0.055
Rotamer outliers (%)	3.17
Overall Molprobity score	1.82
Average B factor (Å ²)	56.0
Protein	84.57
Ramachandran plot	
Most favoured (%)	97.4
Additionally allowed	2.0
Disallowed (%)	0.6
PDB deposition	8bt1

Statistics for the highest-resolution shell are shown in parentheses.

Table S4 SAXS experimental details

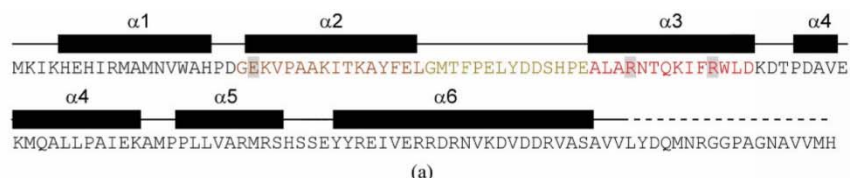
	YdaT	YdaT ¹⁻⁹⁶	YdaT-OM
<i>(a)</i> Sample details			
Loading volume	45 µl	45 µl	45 µl
Injected concentration	10 mg ml ⁻¹	10 mg ml ⁻¹	~8 mg ml ⁻¹ *
Flow rate	0.3 ml min ⁻¹	0.3 ml min ⁻¹	0.16 ml min ⁻¹
Solvent composition	20 mM Tris-HCl, 200 mM NaCl, pH 8	20 mM Tris-HCl, 200 mM NaCl, pH 8	20 mM Tris-HCl, 200 mM NaCl, pH 8
<i>(b)</i> SAS data collection parameters			
Source	SWING beamline, SOLEIL	SWING beamline, SOLEIL	BM29 beamline, ESRF
Sample configuration	In-line HPLC, quartz capillary cell	In-line HPLC, quartz capillary cell	In-line HPLC, quartz capillary cell
Wavelength (Å)	1.03	1.03	0.99
<i>q</i> -measurement range (Å ⁻¹)	0.0037 – 0.52	0.0037 – 0.51	0.0044 – 0.52
Exposure time, number of exposures	0.990 s frames	0.990 s frames	2.0 s frames
Sample configuration	In-line HPLC, quartz capillary cell	In-line HPLC, quartz capillary cell	In-line HPLC, quartz capillary cell
Sample temperature (°C)	15	15	15
<i>(c)</i> Software			
Data reduction	Foxtrot 3.5.10-3979	Foxtrot 3.5.10-3979	DAHU, CHROMIXS
Basic analyses: Guinier, <i>P(r)</i> , Porod volume <i>V_P</i>	Primus from the ATSAS 3.03 package	Primus from the ATSAS 3.03 package	Primus from the ATSAS 3.03 package
Atomic structure modelling	Xplor-NIH v 2.49	Xplor-NIH v 2.49	Xplor-NIH v 2.49
<i>(d)</i> Structural parameters			
Guinier analysis:			
<i>I</i> (0) (cm ⁻¹)	0.058 +/- 0.00004	0.021 +/- 0.00005	5.78 +/- 0.016
<i>R_g</i> (Å)	34.79 +/- 0.03	24.06 +/- 0.09	41.88 +/- 0.17
<i>q</i> -range (Å ⁻¹)	0.017 - 0.037	0.010 - 0.074	0.011 – 0.031
Quality of fit estimation (from AUTORG)	0.875	0.928	0.745
<i>P(r)</i> analysis:			
<i>I</i> (0) (cm ⁻¹)	0.06 +/- 0.00003	0.02 +/- 0.00004	5.77 +/- 0.013

R_g (Å)	34.94 +/- 0.03	24.75 +/- 0.08	42.13 +/- 0.1
d_{\max} (Å)	119.9	82.19	128.13
q -range (Å ⁻¹)	0.017 - 0.252	0.010 - 0.461	0.011 - 0.191
χ^2 (total estimate from <i>GNOM</i>)	0.8721	0.8315	0.9065
Volume (V_p , Å ³)	129558	28973	193022
<hr/>			
(e) Atomistic modelling			
Method	Simulations in Xplor-NIH based on crystallographic coordinates of the tetramer YdaT	Simulations in Xplor-NIH based on crystallographic coordinates of the N-terminal YdaT domain	Simulations in Xplor-NIH based on crystallographic coordinates docked to DNA model
q -range for fitting (Å ⁻¹)	0.00620 - 0.24990	0.00660 - 0.24990	0.01110 - 0.22040
χ^2 value/range	1.684	0.99	1.418
<hr/>			
(f) Deposition			
Deposition IDs	SASDQB9	SASDQD9	SASDQE9

* Approximate value - see Material and Methods for details regarding sample preparation

Table S5 Operator fragments used for ITC, native MS and SAXS. The complete and incomplete inverted repeats are underlined.

oligonucleotide	sequence 5' -> 3'
O _M	TCATG <u>CTTGA</u> TTTCAT <u>GAATCA</u> ACTCCAT
O _L	CCGG <u>GATGC</u> GCCCAGAC <u>ATTCA</u> TGCC
O _R	GATA <u>AGCATG</u> CACTACA <u>ATCAC</u> CTTC
O _{LM}	GG <u>ATGCG</u> CCCAGAC <u>ATTCA</u> TGCCATGCCGATGTGTT <u>CATGCTTGA</u> TTTCAT <u>GAATCA</u> CT
O _{MR}	G <u>CTTGATTTC</u> CAT <u>GAATCA</u> ACTCCATCAGATA <u>AGCATG</u> CACTACA <u>ATCAC</u> CT



Uniprot ID	Organism	E-value
YdaT O157:H7	<i>E. coli</i> O157:H7	-
A0A653FVG1	Escherichia phage Evi	2.1 E-84
Q8X577	<i>E. coli</i> O157:H7	2.6 E-85
Q8X4Y2	<i>E. coli</i> O157:H7	1.3 E-96
Q8X551	<i>E. coli</i> O157:H7	5.8 E-82
Q8X4T2	<i>E. coli</i> O157:H7	2.0 E-82
Q8X4U7	<i>E. coli</i> O157:H7	3.3 E-81
A0A482IJ73	Klebsiella phage ST405-OXA48...	7.5 E-48
D4E7H5	Serratia odorifera DSM 4582	5.4 E-47
A0A2V1H7Z6	<i>Serratia</i> sp. S1B	2.0 E-13
A0A089PWY9	Cedecea neteri	3.4 E-11
A0A1JCLW6	<i>Sodalis</i> sp. TME1	5.2 E-11
Q0A2V5I7	<i>Beauveria bassiana</i> D1-5	1.2 E-9
Q0A2G8EK32	<i>Erwinia</i> sp. OLSSP12	1.4 E-10
A0A6M3AUN3	Escherichia phage Rac	1.1 E-7
Q7N1J8	<i>Photorhabdus laumondii</i>	7.7 E-6
A0A0H2UYD3	<i>Shigella flexneri</i>	2.5 E-5
P76064	<i>E. coli</i> (strain K12)	4.9 E-5
COAW01	<i>Proteus penneri</i> ATCC 35198	1.1 E-5
Q8X8R7	<i>E. coli</i> O157:H7	3.5 E-5
A8AHR8	Citrobacter koseri	3.6 E-5
A0A4P8YJA6	<i>Izakhiella</i> sp. KSNA2	1.1 E-3
A0A378CLT9	<i>Klebsiella pneumoniae</i>	1.1 E-3
A0A1D3BMJ2	Enterobacter asburiae	1.1 E-3
H8C162	Pectobacterium phage ZF40	1.5 E-3
A0A0U2RXZ9	Escherichia phage Rac-SA53	0.015
A0A2I5THJ6	<i>Serratia</i> sp. (strain ATCC 39006)	0.013
A0A090VY18	Pseudescherichia vulneris	8.3 E-3
G8C7U3	<i>Escherichia</i> phage HK639	5.8 E-3
K7P7P2	Enterobacteriophage HK225	0.011
K7PJ7	Enterobacteriophage mEp237	0.010
A0A090V4F7	Pseudescherichia vulneris NB...	0.053
EOSLW2	Dickeya dadantii (strain 3937)	0.11
A0A653FQP0	Escherichia virus Lambda_4C10	6.0
A6T899	<i>Klebsiella pneumoniae</i>	8.3
U3C976	<i>Vibrio</i> <i>azorensis</i> NBRC 104587	2.2
A0A481W3Q0	Escherichia phage PHB10	
A0A653FURO	Escherichia phage mEp460_ev081	

(b)

Figure S1 YdaT sequence. **a.** Comparison of the immunity region of bacteriophage λ and prophage CP-933P. **b.** Amino acid sequence of YdaT with the secondary structure elements indicated. The HTH motif is coloured with helix α 2 in orange, the recognition helix α 3 in red and the connecting loop in dark yellow. Residues Glu21, Arg53 and Arg60 are highlighted on a grey background **c.** Sequence alignment of the HTH motif of 38 selected homologs that were picked up using a BLAST search. Picked-up sequences that were (likely) incomplete or that according to Alphafold2 predictions deviate from the POU domain structure were removed. To obtain the best possible alignment of the α 2- α 3 loop region, Alphafold2 predictions were used as a guide. Colouring is as in panel a.

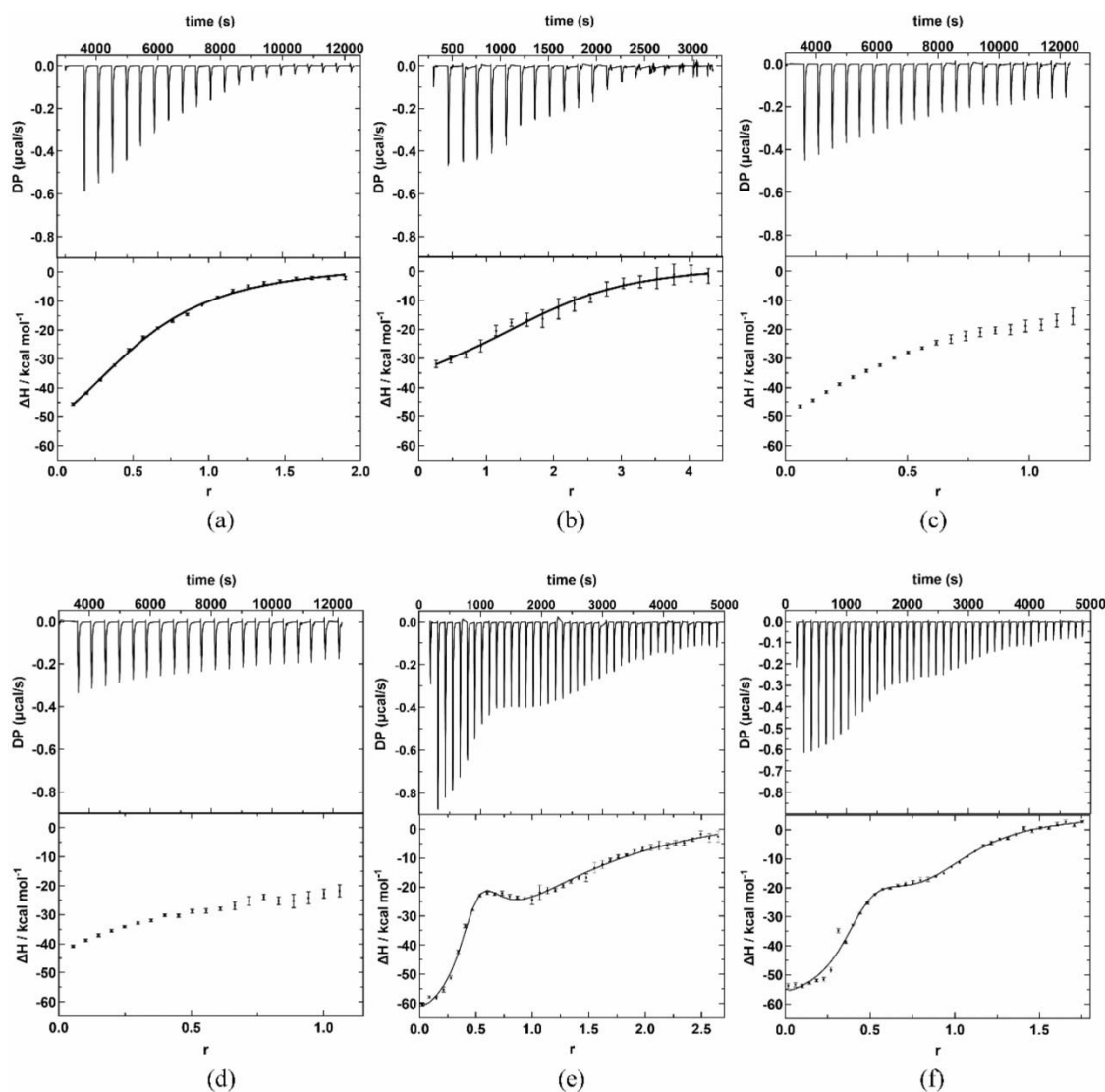


Figure S2 ITC analysis of DNA binding for YdaT at 25 °C. Upper panels show thermograms with subtracted baseline and lower panels integrated heats of injections per mole of injected protein or DNA. Black curves represent fitted model function. All molar ratios were calculated for YdaT as a tetramer. **a.** YdaT titrated into O_M solution. **b.** Reverse titration of O_M into YdaT. A model function for two independent non-equivalent binding sites was fitted globally to both titrations of YdaT and O_M yielding a single set of thermodynamic parameters. **c.-d.** Titrations of YdaT into O_L and O_R . **e.-f.** YdaT titrated into O_{LM} and O_{MR} .

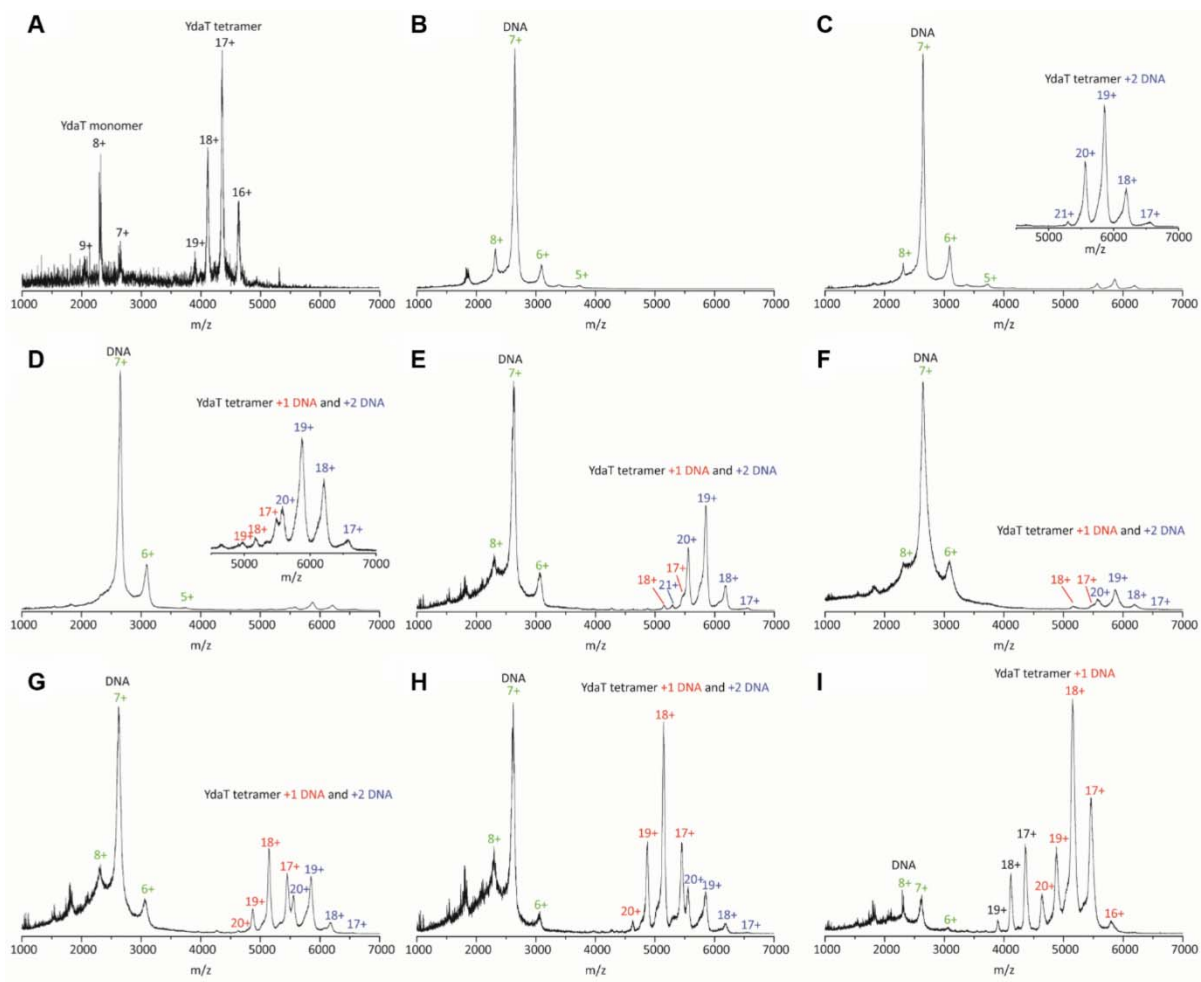


Figure S3 Native mass spectrometry of YdaT titrated with O_M . All concentrations are calculated for YdaT tetramer. **a.** Native MS spectrum of a free YdaT at a concentration of 2.5 μM (tetramer equivalents). **b.** Native MS spectrum for a free O_M duplex at a concentration of 5 μM. **c.-i.** Titration of O_M into 2.5 μM YdaT. O_M concentrations are in following order: 15 μM, 10 μM, 5 μM, 3.33 μM, 2.5 μM, 2 μM and 1.67 μM. When YdaT is oversaturated with O_M (c) only a species corresponding to YdaT₄-2x O_M is observed next to an excess of free O_M . With increasing protein to DNA ratio (d-h) a mixture of YdaT₄-2x O_M and YdaT₄- O_M is observed with the latter increasing. At a 1.5x excess of protein (i) only a species YdaT₄- O_M is observed in addition to free protein.

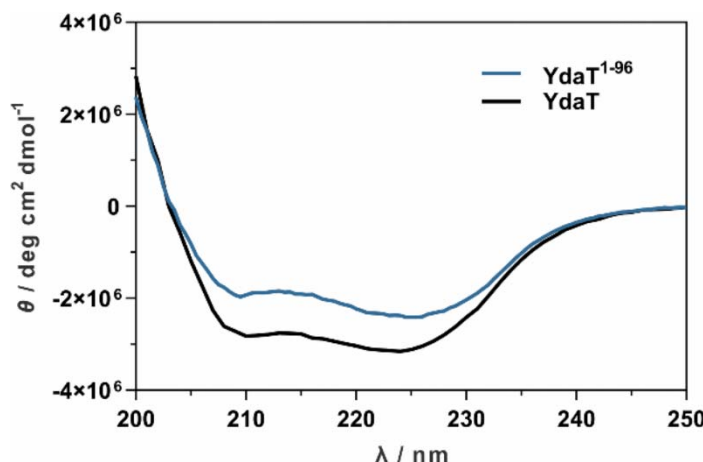


Figure S4 CD spectroscopy. CD spectra are shown for wild-type YdaT (black) and YdaT¹⁻⁹⁶ (blue), and were normalized in terms of molar equivalents of monomers. All proteins show clear evidence for a folded structure dominated by α -helix (two minima at approximately 222 and 208 nm). The somewhat smaller signal for YdaT¹⁻⁹⁶ reflects the absence of the C-terminal helix α 6.

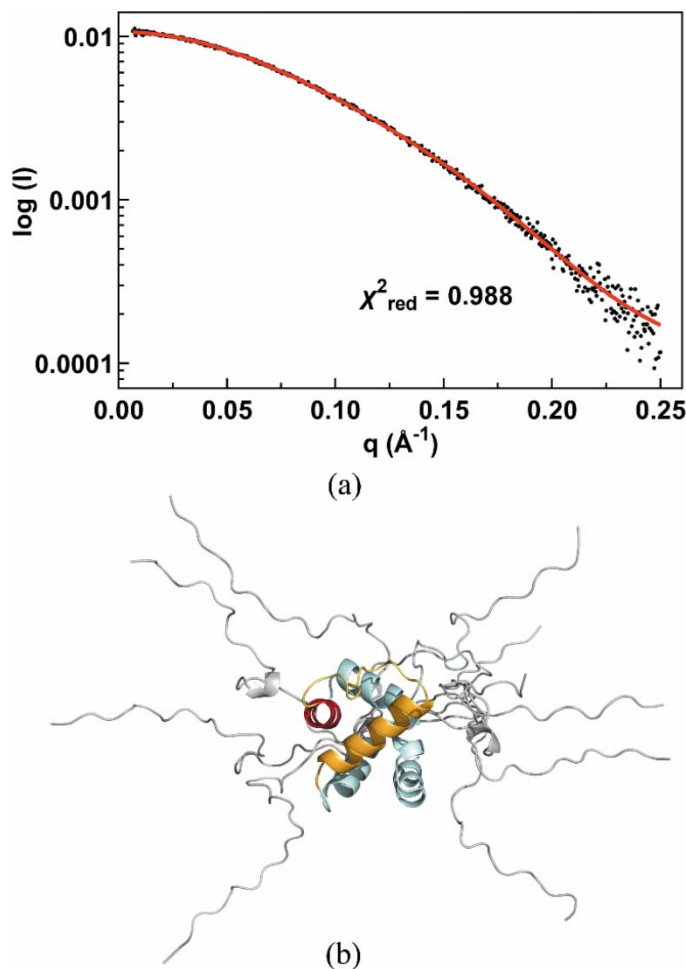


Figure S5 SAXS analysis of the YdaT mutants. **a.** Experimental SAXS data of YdaT¹⁻⁹⁶ (black) with the calculated curve for the best ensemble of the protein (10 models, $\chi^2 = 0.983$) superimposed in red. **b.** Superimposed ensemble of YdaT¹⁻⁹⁶ models showing multiple orientations of the N-terminal His-tag and a rigid POU domain.